

Article

## Unusual Behaviour of Donor-Acceptor Stenhouse Adducts (DASA) in Confined Space of a Water Soluble PdII8 Molecular Vessel

Rupak Saha, Anthonisamy Devaraj, Soumalya Bhattacharyya,  
Soumik Das, Ennio Zangrando, and Partha Sarathi Mukherjee

*J. Am. Chem. Soc.*, **Just Accepted Manuscript** • DOI: 10.1021/jacs.9b03924 • Publication Date (Web): 03 May 2019

Downloaded from <http://pubs.acs.org> on May 3, 2019

### Just Accepted

“Just Accepted” manuscripts have been peer-reviewed and accepted for publication. They are posted online prior to technical editing, formatting for publication and author proofing. The American Chemical Society provides “Just Accepted” as a service to the research community to expedite the dissemination of scientific material as soon as possible after acceptance. “Just Accepted” manuscripts appear in full in PDF format accompanied by an HTML abstract. “Just Accepted” manuscripts have been fully peer reviewed, but should not be considered the official version of record. They are citable by the Digital Object Identifier (DOI®). “Just Accepted” is an optional service offered to authors. Therefore, the “Just Accepted” Web site may not include all articles that will be published in the journal. After a manuscript is technically edited and formatted, it will be removed from the “Just Accepted” Web site and published as an ASAP article. Note that technical editing may introduce minor changes to the manuscript text and/or graphics which could affect content, and all legal disclaimers and ethical guidelines that apply to the journal pertain. ACS cannot be held responsible for errors or consequences arising from the use of information contained in these “Just Accepted” manuscripts.



# Unusual Behaviour of Donor-Acceptor Stenhouse Adducts (DASA) in Confined Space of a Water Soluble Pd<sub>8</sub> Molecular Vessel

Rupak Saha<sup>1</sup>, Anthonisamy Devaraj<sup>1§</sup>, Soumalya Bhattacharyya<sup>1§</sup>, Soumik Das<sup>1</sup>, Ennio Zangrando<sup>2</sup> and Partha Sarathi Mukherjee<sup>1\*</sup>

<sup>1</sup>Department of Inorganic and Physical Chemistry, Indian Institute of Science, Bangalore 560012, India

<sup>2</sup>Department of Chemical and Pharmaceutical Sciences, University of Trieste, Trieste 34127, Italy

**ABSTRACT:** Donor-Acceptor Stenhouse Adducts (**DASA**) are new generation photochromic compounds discovered in recent past. **DASA** exist normally in open form (blue/violet) and readily convert to cyclic (light yellow/colourless) zwitterionic form reversibly in presence of green light in toluene/dioxane. In aqueous medium, the open form is not stable and converts to the cyclic zwitterionic form irreversibly. We report here a new self-assembled Pd<sub>8</sub> molecular vessel (**MV**) that can stabilize and store the open form of **DASA** even in aqueous medium. Reaction of 90° acceptor *cis*-(tmeda)Pd(NO<sub>3</sub>)<sub>2</sub> (**M**) [tmeda = N,N,N',N'-tetramethylethane-1,2-diamine] with a symmetric tetraimidazole donor (**L**, 3,3',5,5'-tetra(1*H*-imidazol-1-yl)-1,1'-biphenyl) in 2:1 molar ratio yielded a water soluble [8+4] self-assembled M<sub>8</sub>L<sub>4</sub> molecular barrel (**MV**). This barrel (**MV**) is found to be a potential molecular vessel to store and stabilize the open forms of **DASA** in aqueous medium over the more stable zwitterionic cyclic form, while in absence of the barrel the same **DASA** exist in cyclic zwitterionic form in aqueous medium. The hydrophobic interaction between the cavity and the open-form of **DASA** molecules benefits to reach an out of equilibrium or reverse equilibrium state in aqueous medium. Presence of excess molecular vessel (**MV**) could even drive the conversion of stable cyclic form to open form in aqueous medium. The host-guest complex is stable upon irradiating with green light. To the best of our knowledge, this is the first successful attempt to stabilize the open form of **DASA** molecules in aqueous medium and the first report on the fate of **DASA** in confined space discrete molecular architecture. Furthermore, the molecular vessel has been utilized for catalytic Michael addition reactions of a series of nitrostyrene derivatives with 1,3-indandione in aqueous medium.

## Introduction

Light-driven photo-switching molecules have been of great interest in current research due to their wide applications in light-mediated catalysis, photo-responsive materials, selective drug delivery in biological systems, molecular electronics and so on.<sup>1</sup> Azobenzenes, spiropyrans, dithienylethenes and few others<sup>2</sup> are the major contributors in the field of light-driven photoisomerization related applications. The easy conversion between the two photo-switching forms of these molecules in presence of UV light makes them easy to handle and selective in nature for various applications. However, in order to exhibit photochromism in low energy visible light compared to the potentially harmful UV light,<sup>3</sup> a new class of photochromic molecules was reported in 2014, called donor-acceptor Stenhouse adducts (**DASA**).<sup>4</sup> These molecules photoisomerize from coloured neutral open forms to colourless zwitterionic cyclic forms with irradiation of visible light (Scheme 1) in organic solvents like toluene and dioxane in a reversible manner. Higher molar absorptivity, reversible and effective photo-switching under visible light, a high degree of fatigue resistance, and the simple synthetic procedure make the **DASA** more attractive to chemists than many other competitive photo-switching materials. In this short period, the **DASA** molecules found an intriguing place in the field of polymer science such as temperature localization for bullet impacts in explosives, targeted drug release by light-triggered micelle collapse and controlling wettability.<sup>5</sup>

**Scheme 1. General photo-switching behaviour of DASA molecules. DASA1 and DASA2 are the two molecules which are investigated in this study.**



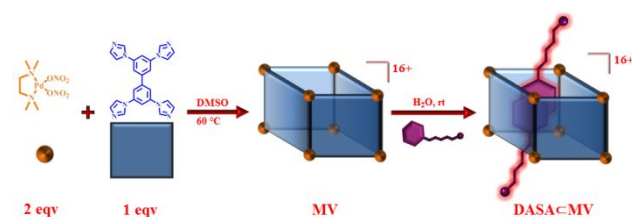
Till date, the reversible photo-switching nature of **DASA** has been restricted to polymer matrices or in solvents such as toluene and dioxane. In dichloromethane and other halogenated solvents thermal cyclic to linear equilibrium was observed to be dominant along with very limited linear to cyclic photoisomerization making the open **DASA** form more stable in these solvents. On the contrary, irreversible linear to cyclic switching has been observed in protic solvents like methanol and water where the ring closed (cyclic zwitterionic) form is stabilized under heating/or in the dark. Thus reversible photo-switching of these **DASA** molecules is restricted in very limited solvents.<sup>4,6</sup> However, the presence of molecular containers may shift the irreversible cycle in the reverse direction by stabilizing the unstable components.<sup>7</sup>

Molecular containers such as crown ethers, cavitands, and self-assembled molecular architectures<sup>8</sup> have shown much versatility and altered the conditions of bringing stability of

many unstable or reactive species and changed the reaction rates.<sup>9</sup> Particularly, the evolution of metal-ligand coordination bonding has become an advance tool for the synthesis of numerous self-assembled supramolecular architectures. The mild reaction conditions and the predesigning aspects of the final assembly make the coordination driven self-assembly superior over the other self-assembly methods. In recent time, coordination driven self-assembly has been used to design molecular vessels for stabilization of unstable conformers, catalysis, separation and host-guest chemistry.<sup>10</sup> The main foundations for these versatile applications of the self-assembled molecular vessels originates due to their easy handling and easy tunabilities by simply changing the donor or acceptor lengths to control the rigidity of the final architectures.

Herein, we report the synthesis and characterization of a new water-soluble tetrafacial molecular vessel (**MV**) obtained via metal-ligand self-assembly of a 90° acceptor *cis*-(*tmeda*)Pd(NO<sub>3</sub>)<sub>2</sub> (**M**) [*tmeda* = N,N,N',N'-tetramethylethane-1,2-diamine] with a symmetric tetraimidazole donor **L** (**L** = 3,3',5,5'-tetra(1*H*-imidazol-1-yl)-1,1'-biphenyl) (Scheme 2). The molecular vessel was characterized by NMR, ESI-MS and single crystal X-ray diffraction studies.

**Scheme 2. Self-assembly of the molecular vessel MV and the unusual stabilization of open form of DASA molecules in aqueous medium.**



The confined nanospace of the barrel stabilized the **DASA** in open form in aqueous medium. While the open form of **DASA** readily converts irreversibly to cyclic form in aqueous medium, stabilization of open form in aqueous medium in presence of the molecular vessel is unique. The open form remains stable in presence of molecular vessel even upon irradiation with visible or green light, a feature which is again a reverse observation of what we see in toluene/dioxane. While the conversion of open form to cyclic form in aqueous medium is irreversible in absence of the molecular barrel, we could convert cyclic form to open form of **DASA** even in aqueous medium in presence of the molecular vessel **MV** (though the process was very slow). Apart from unusual stabilization of the open forms of **DASA** molecules in aqueous medium, **MV** was found to encapsulate other water insoluble compounds like nitrostyrene derivatives, which gave us the eagerness to perform Michael addition reactions in relatively good yields using **MV** in catalytic amount in aqueous medium.

## Results and Discussion

The tetraimidazole donor, 3,3',5,5'-tetra(1*H*-imidazol-1-yl)-1,1'-biphenyl (**L**) was synthesized following the previously reported procedure by treating 3,3',5,5'-tetrabromo-1,1'-biphenyl, imidazole, K<sub>2</sub>CO<sub>3</sub>, and anhydrous CuSO<sub>4</sub> at 180 °C.<sup>11</sup> A clear solution of **L** in DMSO was treated with a DMSO solution of **M** in 1:2 molar ratios and was heated for 12 h at 60 °C. The clear pale-yellow solution upon treating with excess ethyl acetate resulted an off-white solid in good

yield. The solid was dissolved in D<sub>2</sub>O and <sup>1</sup>H NMR was recorded to obtain a clear NMR spectrum containing a single set of the tetraimidazole peaks. The aromatic proton peaks were assigned with the support of <sup>1</sup>H <sup>1</sup>H COSY NMR spectroscopy (Figures S1-S2). Furthermore, diffusion ordered spectroscopy (DOSY) also confirmed the formation of a single self-assembled molecular species **MV** (Figure S3). The composition of **MV** was specifically determined by the electrospray ionisation mass spectroscopy (ESI-MS). The PF<sub>6</sub> analogue of the self-assembled **MV** was prepared by mixing an aqueous solution of **MV** with excess KPF<sub>6</sub>. The PF<sub>6</sub> analogue was solubilized in acetonitrile and ESI-MS was recorded. The appearance of prominent peaks and the isotopic distribution patterns of the fragments for the PF<sub>6</sub> analogue at *m/z* = 1779.4772 for [**MV**-3PF<sub>6</sub>]<sup>3+</sup>, 1298.3660 for [**MV**-4PF<sub>6</sub>]<sup>4+</sup>, 1009.3091 for [**MV**-5PF<sub>6</sub>]<sup>5+</sup> and 817.2660 for [**MV**-6PF<sub>6</sub>]<sup>6+</sup> confirmed the formation of a M<sub>8</sub>L<sub>4</sub> species (Figure S4). The NMR and ESI-MS studies hinted the formation of a molecular barrel, however the exact geometry of **MV** was required to understand the nature and dimensions of the cavity. We were successful to grow single crystals of the PF<sub>6</sub> analogue of **MV** by diffusing acetone in to its DMSO solution. The single crystal structure analysis revealed the formation of a tetragonal barrel, which crystallizes in tetragonal system, space group *P4*<sub>2</sub>/*n*. The solid-state structure revealed that in the molecular barrel the tetraimidazole donor is slightly twisted being roughly of 43° the dihedral angle between the biphenyl rings. This feature induces two opposite corners of the molecular vessel of the acceptor units to be upward (compared to the other two at opposite corners) in the open faces. The distances between the two opposite corners are roughly 20.5 and 13.8 Å for Pd(1)-Pd(1'') and Pd(2)-Pd(2''), respectively, whereas adjacent Pd(1)-Pd(2) atoms are 8.1 Å apart, (Figure 1).

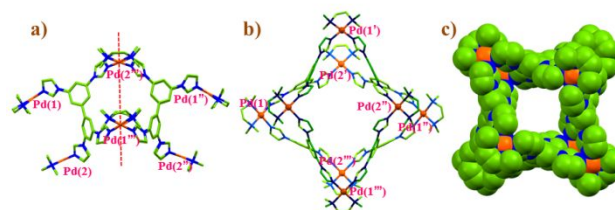


**Figure 1.** SCXRD structure of the molecular vessel **MV**: (a) Side view (stick model) showing two Pd atoms located upward in the open face; (b) view down crystallographic 4<sub>2</sub> axis; (c) space-filled model [Colour codes: C (green), N (blue), Pd (orange)]. Hydrogen atoms, counter anions and solvent molecules were omitted for the sake of clarity.

The crystal structure showed the presence of two open windows having a barrel-shaped hydrophobic cavity, which marks **MV** as a perfect choice for encapsulation of water insoluble guest molecules of various sizes and shapes. **DASA** molecules have gained a lot of interest since their recent discovery in 2014 due to their photochromic behaviour in low energy visible light. Both the **DASA1** and **DASA2** are soluble in common organic solvents and show reversible photochromic behaviour in toluene and dioxane. The open forms of **DASA** are generally blue or violet in colour which upon irradiation with green light slowly becomes pale yellow via converting to the cyclic form. The cyclic form readily reverts back to the open form by keeping the solution in dark

or upon heating. On the contrary, their stability in water or methanol as the open form diminishes with time and the zwitterionic cyclic form gains solidity extensively (Figure S20). Therefore, to check the stability of the open form of the **DASA** in presence of the molecular vessel as host, we treated the pale-yellow aqueous solution of **MV** with the excess **DASA** compounds in water for 2 days and UV-vis spectra were recorded on the resulted red solutions. Generally, the open form of the **DASA** shows an absorption peak at around 540 nm and the zwitterionic cyclic form gives an absorption band at around 264 nm. Surprisingly, the UV-vis spectra of the host-guest solution mixture showed broad band near 509 nm and 512 nm confirming the presence of the open forms of the **DASA1** and **DASA2** molecule respectively, which was not observed when similar conditions were maintained in absence of the molecular vessel (Figure 2). This observation hints that the molecular vessel **MV** can provide significant stability to arrest the open form in aqueous medium.

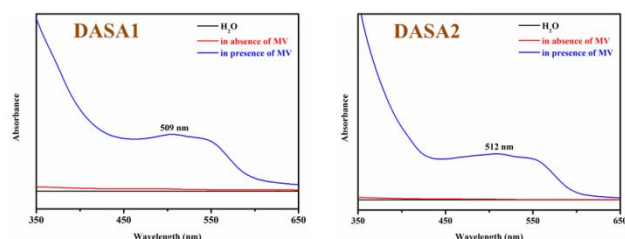


**Figure 2:** Comparison of UV-visible spectra of the open form of **DASA** molecules in presence of **MV**, and in absence of **MV** in aqueous medium.

Additionally, the host-guest complexation was confirmed by performing  $^1\text{H}$ , DOSY and NOESY NMR in  $\text{D}_2\text{O}$  at room temperature (Figures S9-S13). The  $^1\text{H}$  NMR spectra confirmed the formation of the host-guest complex (**DASA** $\subset$ **MV**) revealing a complex spectrum compared to the simple  $^1\text{H}$  NMR of the host **MV**. The aromatic region appeared broad due to the lack of symmetry in the host-guest complex and made it difficult to interpret the results. However, the peak at 9.04 ppm, assigned to the imidazole, shifts downfield to 9.11 ppm inferring the formation of **DASA1** $\subset$ **MV** complex. Additionally, the peak at 2.99 ppm due to the presence of the N methyl protons shifted upfield compared to its proton NMR spectrum recorded in  $\text{CDCl}_3$  (Figure 3). The proton shifts are affected by the interactions between the host and guest molecules within the **DASA1** $\subset$ **MV** complex. The stability of the host and also the guest molecule was checked by extracting the deuterated aqueous solution of the host-guest complex **DASA1** $\subset$ **MV** with  $\text{CDCl}_3$ , which transformed the red aqueous solution back into a pale-yellow solution. Furthermore, the proton NMR of both the layers was checked and confirmed that the  $\text{D}_2\text{O}$  layer contained the molecular vessel **MV** and the  $\text{CDCl}_3$  layer showed the presence of **DASA1**. The  $^1\text{H}$  DOSY spectrum confirmed the formation of a single host-guest complex **DASA1** $\subset$ **MV**. The ratio of the host-guest complex was determined by calculating the proton integral values of the imidazole peak of the host molecule and the N methyl protons peak of the guest molecule revealing that each **MV** host molecule can encapsulate two **DASA1** molecules.

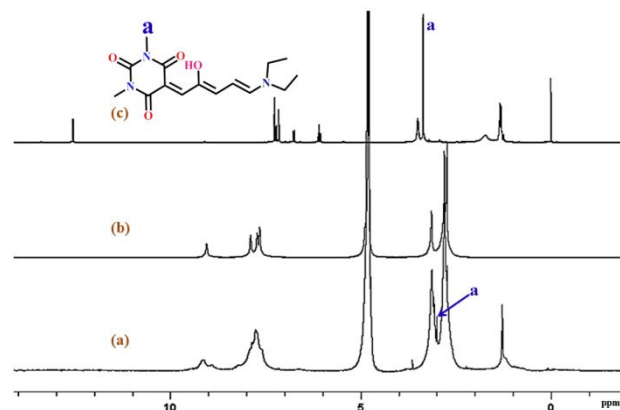
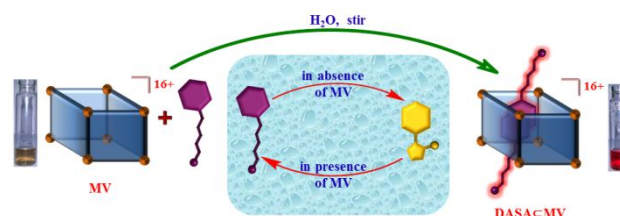


**Figure 3:**  $^1\text{H}$  NMR of (a) **DASA1** $\subset$ **MV**, (b) **MV** recorded in  $\text{D}_2\text{O}$  and (c) linear/open form of **DASA1** recorded in  $\text{CDCl}_3$  at 298 K.

Similar observations were also noted for the **DASA2** molecule. Moreover, we prepared another solution of the host-guest complex **DASA2** $\subset$ **MV** by taking excess of guest molecules. The proton spectra gave a similar complicated NMR with two sharp doublets at 7.85 and 6.66 ppm confirming the presence of the cyclic form of the **DASA2** molecule (Figure 4) along with **DASA2** $\subset$ **MV**. The DOSY spectra showed the presence of two distinguishable bands: one corresponding to the host-guest complex **DASA2** $\subset$ **MV** and the other representing the free cyclic form of the **DASA2** (Figures S14-S15). Here also the proton NMR spectra confirmed the formation of a 1:2 host-guest complex **DASA2** $\subset$ **MV**. While the cyclic form of **DASA** is stable in aqueous medium and doesn't go back to open form in absence of barrel, addition of excess molecular vessel **MV** converted the cyclic form of **DASA** to open form by forming host-guest (Figures S18-S19) complex. To the best of our knowledge, the present observation represents the first example of cyclic-form to open-form transformation of **DASA** in aqueous medium (Scheme 3).

### Scheme 3. Encapsulation of **DASA** molecules into the cavity of **MV** to give a red solution



To our surprise the host-guest complex solutions (**DASA** $\subset$ **MV**) did not have any effect upon exposure to visible light and remained unchanged for several months, as confirmed by NMR analysis (Figures S16-S17).

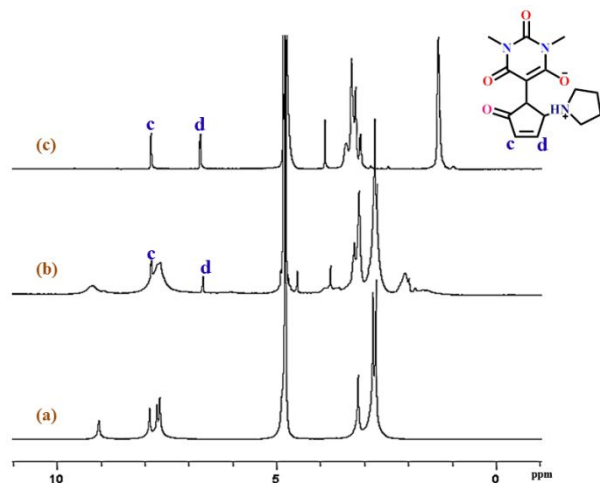


**Figure 4:** <sup>1</sup>H NMR of (a) MV, (b) DASA2:CMV in presence of excess guest, (c) cyclic DASA2 recorded in D<sub>2</sub>O at 298 K.

Furthermore, to accomplish the encapsulation of the DASA molecules, we carried out a control experiment using three equivalents and one equivalent of the DASA molecules with respect to one equivalent of MV by stirring at room temperature for 7 days. Afterwards, the UV-vis spectra of the centrifuged clear solutions were recorded and compared with the UV-vis spectra of MV and the cyclic form of DASA in aqueous medium (Figure 5). The appearance of a shoulder near 262 nm confirmed the presence of the cyclic form of DASA molecules when we used three equivalents DASA molecules, such observations were absent when one equivalent of DASA molecule was used. The shoulder appeared near 262 nm due to the presence of excess DASA molecules which got converted to its cyclic form with time. Thus, indicating that MV acts as a suitable molecular container to stabilize the open form of the DASA molecules.

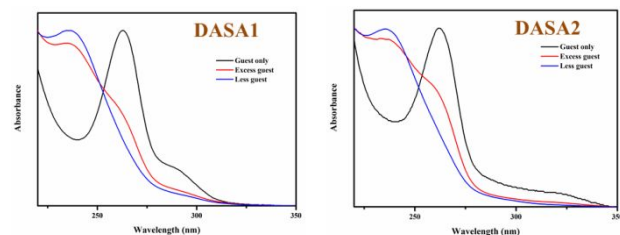


**Figure 5.** Comparative UV-visible spectra of the DASA cyclic form (guest only), (1:1) DASA:MV (less guest) and (3:1) DASA:MV (excess guest) showing the formation of host-guest complexes.

Several attempts to grow single crystals of DASA1:CMV by slow evaporation and vapour diffusion technique from the aqueous solution of the host-guest complex were unsuccessful. However, the geometry of the complex DASA1:CMV was optimized by DFT method by placing two DASA molecules in head to tail fashion inside the cavity of the molecular vessel MV (Figure 6). Lastly, to comprehend the optical property, time-dependent DFT calculation was carried out on the energy-optimized structure to give an UV/vis spectrum having a  $\lambda_{\text{max}}$  at 548 nm, which is fairly close to the experimental one. Similarly, for the case of DASA2 the energy-optimized structure showed an UV/vis spectrum having  $\lambda_{\text{max}}$  at 564 nm (Figure S21).

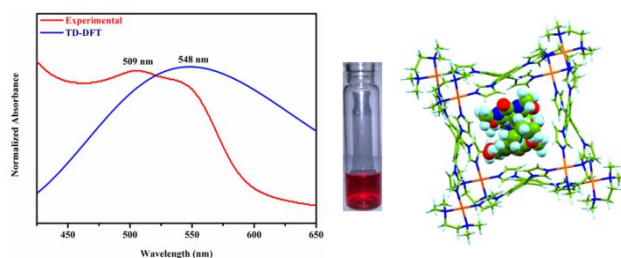


**Figure 6.** Comparison of experimental and theoretical (TD-DFT) UV/vis spectra (left) and the energy-optimized geometry (right) of DASA1:CMV. Colour codes: Hydrogen (sky blue), Carbon (green), Nitrogen (blue), Palladium (Orange).

Additionally, to explore the hydrophobic cavity of the molecular vessel as reaction chamber, nitrostyrene derivatives (1a-1g) were treated with the deuterated aqueous solution of MV. After centrifuging <sup>1</sup>H NMR for the host-guest (guest = 1d) complex was recorded with the clear solution. The proton NMR spectrum revealed that the peak corresponding to the imidazole peak at 9.04 ppm shifted downfield to 9.18 ppm similar like the DASA molecules. In addition, new peaks appeared between 6.55-5.78 ppm resulting from the upfield shift of the aromatic protons of the nitrostyrene 1d. The DOSY NMR showed a single diffusion band concluding the presence of a single host-guest complex (1d:CMV). The proton NMR integral calculations revealed that the host-guest complex (1d:CMV) constitutes of two nitrostyrene guest molecules inside MV which is similar to the DASA molecules (Figures S22-S27). This is very appropriate as the nitrostyrene molecules hold a similar backbone like the DASA molecules only difference being a shorter tail attached to the hexagon moiety. Michael addition reactions of 1,3-indandione as a nucleophile have been utilized to prepare many of its derivatives which have vast applications in the biological field.<sup>12</sup> Nitrostyrene derivatives being good Michael acceptors, can provide us a wide range of various functionalized Michael adducts with 1,3-indandione. However, most reported methods use acid catalysts in organic solvents which also form unwanted byproducts due to plausible formation of condensed products.<sup>13</sup> Thus continuous efforts for new and effective methods are being given for the synthesis of Michael adducts with 1,3-indandione and nitrostyrenes. After the confirmation of the encapsulation of different nitrostyrenes inside the molecular vessel, we carried out supramolecular catalysis in aqueous medium maintaining a catalytic amount of MV. Nitrostyrene 1a was treated with 1,3-indandione in presence of 5 mol% MV in 1 mL aqueous medium and the mixture was stirred for 30 min at room temperature. The reaction mixture comprising of Michael adduct (2a) was extracted with CDCl<sub>3</sub> and the <sup>1</sup>H NMR spectral analysis of the crude mixture revealed the formation of 89% of product 2a. The product 2a was obtained with high purity by column chromatography (20% ethyl acetate in hexane) and was thoroughly characterized by NMR and HRMS spectroscopy. When the reaction was performed in absence of the cage under identical reaction conditions, 2a was formed in 25% yield. The product enhancement from 25 to 89% in presence of MV highlighted the catalytic involvement of its confined cavity. Furthermore, several reactions were carried out with various derivatives of nitrostyrene and treating with 1,3-indandione in aqueous solution at room temperature (Table 1).

**Table 1. Michael addition of 1a–1f with 1,3-indandione supported by MV**

Entry	Substrate (Ar)	Conversion (%)	Conversion (%)	Time (h)
		without MV*	with MV*	
a	phenyl	25	89	0.5
b	2-chlorophenyl	25	91	2
c	4-chlorophenyl	18	51	6
d	2,4-dichlorophenyl	19	54	24
e	4-methylphenyl	27	72	24
f	4-methoxyphenyl	20	68	24
g	$\alpha$ -naphthyl	5	47	24

\*conversion percentage is based on the  $^1\text{H}$  NMR of the crude sample.

The reaction time and efficiency of the reaction were both varied by the substituent attached on the  $\beta$ -nitrostyrene molecules. The Michael adducts **2a–2g** were commenced via the nucleophilic addition of electron rich 1,3-indandione to  $\beta$ -nitrostyrene derivatives. The host-guest complex presumably gets stabilized through  $\pi$ - $\pi$  interactions within the aromatic walls of **MV** and the guest molecules which can be related from the  $^1\text{H}$ - $^1\text{H}$  NOESY spectra. After the product formation the bulkiness was increased significantly and therefore the molecular barrel was unable to host the product, as a result they were easily released and exchanged with another substrate molecule to carry on the catalytic cycle.

### Conclusions

In conclusion, we report here a new Pd(II) molecular vessel (**MV**) by self-assembly of a tetraimidazole donor with a  $90^\circ$  Pd(II) acceptor utilizing metal-ligand coordination self-assembly. Donor Acceptor Stenhouse Adducts (**DASA**) are new generation photochromic compounds to show photo-switching in visible light. The open form of **DASA** irreversibly converts to cyclic zwitterionic form in aqueous medium. Surprisingly, the newly developed molecular vessel **MV** was found to be potential for storing **DASA** molecules in their open form in aqueous medium. This was possible due to the hydrophobic cavity in **MV**, which makes the open form of **DASA** molecules highly stable in aqueous medium. Though in hydrophobic solvents (toluene/dioxane), the open form of

**DASA** readily converts to cyclic form upon irradiation with green light, after encapsulation the open form was stable even upon prolong irradiation with green light. Thus, the molecular vessel represents a safe container for the open form of **DASA** even in aqueous medium. While the conversion of open to cyclic form of **DASA** in aqueous medium is known to be irreversible, presence of excess **MV** could successfully convert the cyclic form to open form in aqueous form (though the process was very slow). These results represent an unusual behaviour of new generation photochromic **DASA** molecules in molecular vessel in aqueous medium. Furthermore, the hydrophobic cavity of the vessel **MV** is found to be suitable for catalytic Michael addition reactions of a series of nitrostyrene derivatives with 1,3-indandione in good yields.

### Experimental Section

#### Materials and Methods

The reagents and solvents were purchased from reputed commercial suppliers and were handled without any further purification. Bruker 400 MHz spectrometer was used to perform NMR spectra and the described chemical shifts ( $\delta$ ) are in parts per million (ppm) relative to  $(\text{CH}_3)_4\text{Si}$  as an internal standard (0.0 ppm) or proton resonance due to incomplete deuteration of  $\text{D}_2\text{O}$  at 4.79 ppm,  $(\text{CD}_3)_2\text{SO}$  at 2.50 ppm and  $\text{CDCl}_3$  at 7.26 ppm. ESI-MS spectra were carried out on an Agilent 6538 Ultra-High Definition (UHD) Accurate Mass Q-TOF spectrometer. UV-Vis spectra were recorded using Perkin Elmer Lambda-750 spectrophotometer. Tetraimidazole donor (**L**), **DASA1**<sup>4a</sup> and **DASA2**<sup>4b</sup> were synthesized following the reported procedures.

**Synthesis of Molecular Vessel (MV):** The tetraimidazole donor **L** (20 mg, 0.048 mmol) was added to a 5 mL DMSO solution of 33.2 mg *cis*-Pd(*tmeda*)( $\text{NO}_3$ )<sub>2</sub> (**M**) [*tmeda* = *N,N,N',N'*-tetramethylethane-1,2-diamine] (0.096 mmol) and heated for 12 h at 60 °C. Product was isolated as solid upon addition of ethyl acetate. Isolated yield: 49.6 mg (93 %).  $^1\text{H}$  NMR (400 MHz,  $\text{D}_2\text{O}$  at 298 K):  $\delta$  = 9.04 (s, 16H), 7.88 (s, 16H), 7.71 (s, 16H), 7.65 (s, 24H), 3.13 (s, 32H), 2.79 (s, 96H). ESI-MS (*m/z*): Calcd *m/z* = 1779.4973 for [**MV**-3PF<sub>6</sub>]<sup>3+</sup>; 1298.3819 for [**MV**-4 PF<sub>6</sub>]<sup>4+</sup>; 1009.3127 for [**MV**-5 PF<sub>6</sub>]<sup>5+</sup>; 817.2666 for [**MV**-6 PF<sub>6</sub>]<sup>6+</sup>. Found: 1779.4772, 1298.3660, 1009.3091 and 817.2660, respectively.

**Encapsulation of DASA molecules and other Nitrostyrene Derivatives:** 8.9 mg (0.002 mmol) of **MV** was dissolved in 0.5 mL  $\text{D}_2\text{O}$  and the solution was added to 0.006 mmol of the guest molecules separately. The suspension was stirred for 24 h at room temperature and later the solution was centrifuged to obtain the clear solution.

**UV-vis Study for DASA molecules:** For UV-vis study of **DASA** molecules, two solutions containing **DASA** molecules were prepared. In the first one 0.002 mmol **MV** was dissolved in 1 mL water and 0.002 mmol of **DASA** molecules were added (less guest). Secondly, in a similar manner 0.002 mmol **MV** was dissolved in 1 mL water and 0.006 mmol of **DASA** molecules was added (excess guest). In a separate vial 0.006 mmol of **DASA** molecules (blank reaction) was also stirred in 1 mL water at room temperature. The three solutions were then kept under stirring for 7 days. The solutions were diluted in a similar extent and UV-vis spectra were recorded.

**General Procedure for the Catalytic Michael Addition Reactions:** To solid nitrostyrene **1** (0.08 mmol), 3 mL aqueous solution of the **MV** (5 mol %) was added followed by

an addition of 1,3-indandione (0.096 mmol). The mixture was stirred at room temperature for the time periods indicated in Table-1 at room temperature. Then the reaction mixture was extracted with chloroform and further column chromatography was done using silica gel, eluting with 20% ethyl acetate in hexane to afford the pure product **2**, which was characterized by <sup>1</sup>H and <sup>13</sup>C NMR and mass spectroscopy (HRMS).

**2a:** <sup>1</sup>H NMR (400 MHz, CDCl<sub>3</sub>): δ = 7.89-7.74 (m, 4H), 7.15 (s, 5H), 5.34 (dd, 1H), 5.10 (dd, 1H), 4.43 (d, 1H), 3.45 (d, 1H). <sup>13</sup>C NMR (100 MHz, CDCl<sub>3</sub>): δ = 199.45, 197.96, 142.75, 142.72, 136.36, 136.33, 135.71, 129.32, 128.87, 128.69, 123.74, 123.66, 76.70, 55.76, 42.48. HRMS calcd for **2a** [M + H]<sup>+</sup> m/z = 296.0923. Found 296.0894. Elemental Analysis for C<sub>17</sub>H<sub>13</sub>N<sub>1</sub>O<sub>4</sub>: C 69.15, H 4.44, N 4.74. Found: C 68.97, H 4.32, N 4.89.

**2b:** <sup>1</sup>H NMR (400 MHz, CDCl<sub>3</sub>): δ = 7.99-7.84 (m, 4H), 7.39 (d, 2H), 7.19 (s, 2H), 5.17 (dd, 1H), 4.97 (s, 1H), 4.83 (dd, 1H), 3.60 (d, 1H). <sup>13</sup>C NMR (100 MHz, CDCl<sub>3</sub>): δ = 198.06, 197.93, 142.31, 136.52, 136.41, 135.07, 134.62, 130.86, 129.87, 129.42, 127.96, 123.97, 123.89, 75.26, 55.21, 37.95. HRMS calcd for **2b** [M + H]<sup>+</sup> m/z = 330.0533. Found 330.0594. Elemental Analysis for C<sub>17</sub>H<sub>12</sub>N<sub>1</sub>O<sub>4</sub>Cl<sub>1</sub>: C 61.92, H 3.67, N 4.25. Found: C 61.59, H 3.61, N 4.17.

**2c:** <sup>1</sup>H NMR (400 MHz, CDCl<sub>3</sub>): δ = 7.89-7.79 (m, 4H), 7.13-6.96 (m, 4H), 5.44-5.25 (m, 1H), 5.19-5.13 (m, 1H), 4.42-4.18 (m, 1H), 3.44 (d, 1H). <sup>13</sup>C NMR (100 MHz, CDCl<sub>3</sub>): δ = 199.21, 197.62, 142.64, 137.48, 137.44, 136.61, 136.56, 130.31, 129.56, 123.89, 123.77, 76.55, 55.70, 41.73. HRMS calcd for **2c** [M + H]<sup>+</sup> m/z = 330.0533. Found 330.0612. Elemental Analysis for C<sub>17</sub>H<sub>12</sub>N<sub>1</sub>O<sub>4</sub>Cl<sub>1</sub>: C 61.92, H 3.67, N 4.25. Found: C 61.71, H 3.59, N 4.34.

**2d:** <sup>1</sup>H NMR (100 MHz, CDCl<sub>3</sub>): δ = 8.00-7.85 (m, 4H), 7.41-7.35 (m, 2H), 7.18 (dd, 1H), 5.13 (dd, 1H), 4.93 (dd, 1H), 4.84 (dd, 1H), 3.56 (d, 1H). <sup>13</sup>C NMR (100 MHz, CDCl<sub>3</sub>): δ = 197.80, 197.65, 142.27, 136.66, 136.57, 135.48, 135.18, 133.66, 130.67, 130.31, 128.28, 124.03, 124.00, 75.17, 55.07, 37.53. HRMS calcd for **2d** [M + H]<sup>+</sup> m/z = 364.0143. Found 364.0087. Elemental Analysis for C<sub>17</sub>H<sub>11</sub>N<sub>1</sub>O<sub>4</sub>Cl<sub>2</sub>: C 56.07, H 3.04, N 3.85. Found: C 56.21, H 2.94, N 3.62.

**2e:** <sup>1</sup>H NMR (100 MHz, CDCl<sub>3</sub>): δ = 7.90-7.83 (m, 4H), 7.05-6.93 (m, 4H), 6.32 (dd, 1H), 5.08 (dd, 1H), 4.39 (d, 1H), 3.43 (d, 1H), 2.16 (s, 3H). <sup>13</sup>C NMR (100 MHz, CDCl<sub>3</sub>): δ = 199.56, 198.00, 142.80, 138.41, 136.29, 136.27, 132.61, 129.99, 128.72, 123.76, 123.65, 76.88, 55.79, 42.16, 21.39. HRMS calcd for **2e** [M + H]<sup>+</sup> m/z = 310.1079. Found 310.1056. Elemental Analysis for C<sub>18</sub>H<sub>15</sub>N<sub>1</sub>O<sub>4</sub>: C 69.89, H 4.89, N 4.53. Found: C 69.63, H 4.67, N 4.29.

**2f:** <sup>1</sup>H NMR (100 MHz, CDCl<sub>3</sub>): δ = 7.89-7.74 (m, 4H), 7.07 (d, 2H), 6.65 (d, 2H), 5.30 (dd, 1H), 5.09 (dd, 1H), 4.39 (d, 1H), 3.65 (s, 3H), 3.41 (d, 1H). <sup>13</sup>C NMR (100 MHz, CDCl<sub>3</sub>): δ = 199.68, 198.07, 159.67, 142.82, 136.33, 136.29, 130.01, 127.51, 123.74, 123.62, 114.63, 76.99, 55.88, 55.54, 41.87. HRMS calcd for **2f** [M + H]<sup>+</sup> m/z = 326.1028. Found 326.1092. Elemental Analysis for C<sub>18</sub>H<sub>15</sub>N<sub>1</sub>O<sub>5</sub>: C 66.46, H 4.65, N 4.31. Found: C 66.02, H 4.43, N 4.53.

**2g:** <sup>1</sup>H NMR (100 MHz, CDCl<sub>3</sub>): δ = 8.37 (d, 1H), 7.99 (d, 1H), 7.83-7.72 (m, 5H), 7.65 (t, 1H), 7.52 (d, 2H), 7.34 (t, 1H), 5.39 (s, 2H), 4.93 (d, 1H), 3.68 (s, 1H). <sup>13</sup>C NMR (100 MHz, CDCl<sub>3</sub>): δ = 198.95, 198.07, 142.45, 142.39, 136.33, 136.26, 134.52, 133.56, 131.36, 129.48, 129.38, 127.59, 126.63, 125.64, 123.86, 123.82, 123.23, 76.27, 56.20, 35.83.

HRMS calcd for **2g** [M + H]<sup>+</sup> m/z = 346.1079. Found 346.1024. Elemental Analysis for C<sub>21</sub>H<sub>15</sub>N<sub>1</sub>O<sub>4</sub>: C 73.04, H 4.38, N 4.06. Found: C 72.82, H 4.19, N 4.26.

### X-Ray Crystallographic Studies:

Single crystal X-ray diffraction data of **MV** were collected at the X-ray diffraction beamline (XRD1) of the Elettra Synchrotron of Trieste (Italy), with a Pilatus 2M image plate detector and a monochromatic wavelength of 0.700 Å. Complete dataset was collected at 100 K with nitrogen stream and the structure was solved by direct methods using SHELX-2007 software package incorporated in WinGX.<sup>14</sup> The structure was solved by direct methods and Fourier analyses. Then it was refined by the full-matrix least-squares method based on F<sup>2</sup> with all observed reflections using the SHELX-2013<sup>15</sup> program incorporated in WinGX. The non-hydrogen atoms in the main fragment were refined with anisotropic displacement parameters and hydrogen atoms were fixed at geometrical position. SQUEEZE option of PLATON was used at the final cycles of refinement in order to account for the contribution of disordered solvent molecules to the calculated structure factors.

## ASSOCIATED CONTENT

### Supporting Information.

<sup>1</sup>H, <sup>13</sup>C, <sup>1</sup>H-<sup>1</sup>H COSY, <sup>1</sup>H-<sup>1</sup>H NOESY and DOSY NMR spectra, ESI-MS data, crystallographic data of MV in CIF format (CCDC No. 1905284), UV-vis spectra of the molecular vessel (**MV**), Donor-Acceptor Stenhouse Adducts (**DASA**) and the catalyzed products associated with this article are attached.

## AUTHOR INFORMATION

### Corresponding Author

\*psm@iisc.ac.in (P. S. Mukherjee)

### Author Contributions

§ Authors contributed equally

### Notes

The authors declare no competing financial interest.

## ACKNOWLEDGMENT

P.S.M. thanks the SERB (New Delhi) for financial support. A.D. is grateful to UGC (New Delhi) for Dr. D. S. Kothari postdoctoral fellowship. S.B. acknowledges the CSIR, New Delhi for the research fellowship.

## REFERENCES

- (1) (a) Jia, C.; Migliore, A.; Xin, N.; Huang, S.; Wang, J.; Yang, Q.; Wang, S.; Chen, H.; Wang, D.; Feng, B. Covalently bonded single-molecule junctions with stable and reversible photoswitched conductivity. *Science* **2016**, *352*, 1443-1445; (b) Andréasson, J.; Pischel, U. Smart molecules at work—mimicking advanced logic operations. *Chem. Soc. Rev.* **2010**, *39*, 174-188; (c) Liu, D.; Chen, W.; Sun, K.; Deng, K.; Zhang, W.; Wang, Z.; Jiang, X. Resettable, multi-readout logic gates based on controllably reversible aggregation of gold nanoparticles. *Angew. Chem., Int. Ed.* **2011**, *50*, 4103-4107; (d) Andréasson, J.; Pischel, U.; Straight, S. D.; Moore, T. A.; Moore, A. L.; Gust, D. All-photonic multifunctional molecular logic device. *J. Am. Chem. Soc.* **2011**, *133*, 11641-11648; (e) Leydecker, T.; Herder, M.; Pavlica, E.; Bratina, G.; Hecht, S.; Orgiu, E.; Samori, P. Flexible non-volatile optical memory thin-film transistor device with over 256 distinct levels based on an organic

bicomponent blend. *Nature nanotechnology* **2016**, *11*, 769; (f) Stoll, R. S.; Hecht, S. Artificial light-gated catalyst systems. *Angew. Chem., Int. Ed.* **2010**, *49*, 5054-5075; (g) Zhang, X.; Hou, L.; Samori, P. Coupling carbon nanomaterials with photochromic molecules for the generation of optically responsive materials. *Nat. Commun.* **2016**, *7*, 11118; (h) Zheng, Z.-g.; Li, Y.; Bisoyi, H. K.; Wang, L.; Bunning, T. J.; Li, Q. Three-dimensional control of the helical axis of a chiral nematic liquid crystal by light. *Nature* **2016**, *531*, 352; (i) Liu, J.; Bu, W.; Pan, L.; Shi, J. NIR-triggered anticancer drug delivery by upconverting nanoparticles with integrated azobenzene-modified mesoporous silica. *Angew. Chem.* **2013**, *125*, 4471-4475; (j) Lv, G.; Cui, B.; Lan, H.; Wen, Y.; Sun, A.; Yi, T. Diarylethene based fluorescent switchable probes for the detection of amyloid- $\beta$  pathology in Alzheimer's disease. *Chem. Commun.* **2015**, *51*, 125-128; (k) Szymański, W.; Beierle, J. M.; Kistemaker, H. A.; Velema, W. A.; Feringa, B. L. Reversible photocontrol of biological systems by the incorporation of molecular photoswitches. *Chem. Rev.* **2013**, *113*, 6114-6178.

(2) (a) Fredrich, S.; Göstl, R.; Herder, M.; Grubert, L.; Hecht, S. Switching diarylethenes reliably in both directions with visible light. *Angew. Chem., Int. Ed.* **2016**, *55*, 1208-1212; (b) Baroncini, M.; d'Agostino, S.; Bergamini, G.; Ceroni, P.; Comotti, A.; Sozzani, P.; Bassanetti, I.; Grepioni, F.; Hernandez, T. M.; Silvi, S. Photoinduced reversible switching of porosity in molecular crystals based on star-shaped azobenzene tetramers. *Nat. Chem.* **2015**, *7*, 634;

(c) Kumar, K.; Knie, C.; Bléger, D.; Peletier, M. A.; Friedrich, H.; Hecht, S.; Broer, D. J.; Debijs, M. G.; Schenning, A. P. A chaotic self-oscillating sunlight-driven polymer actuator. *Nat. Commun.* **2016**, *7*, 11975; (d) Klajn, R. Spiropyran-based dynamic materials. *Chem. Soc. Rev.* **2014**, *43*, 148-184; (e) Saad, A.; Oms, O.; Dolbecq, A.; Menet, C.; Dessapt, R.; Serier-Braut, H.; Allard, E.; Baczko, K.; Mialane, P. A high fatigue resistant, photoswitchable fluorescent spiropyran-polyoxometalate-BODIPY single-molecule. *Chem. Commun.* **2015**, *51*, 16088-16091; (f) van Dijken, D. J.; Kovaříček, P.; Ihrig, S. P.; Hecht, S. Acylhydrazones as widely tunable photoswitches. *J. Am. Chem. Soc.* **2015**, *137*, 14982-14991;

(g) Liu, Z.; Liu, T.; Lin, Q.; Bao, C.; Zhu, L. Sequential control over thiol click chemistry by a reversibly photoactivated thiol mechanism of spirothiopyran. *Angew. Chem.* **2015**, *127*, 176-180;

(h) Mazzier, D.; Crisma, M.; De Poli, M.; Marafon, G.; Peggion, C.; Clayden, J.; Moretto, A. Helical Foldamers Incorporating Photoswitchable Residues for Light-Mediated Modulation of Conformational Preference. *J. Am. Chem. Soc.* **2016**, *138*, 8007-8018; (i) Kobayashi, Y.; Katayama, T.; Yamane, T.; Setoura, K.; Ito, S.; Miyasaka, H.; Abe, J. Stepwise two-photon-induced fast photoswitching via electron transfer in higher excited states of photochromic imidazole dimer. *J. Am. Chem. Soc.* **2016**, *138*, 5930-5938.

(3) Bleger, D.; Hecht, S. Visible-light-activated molecular switches. *Angew. Chem., Int. Ed.* **2015**, *54*, 11338-11349.

(4) (a) Helmy, S.; Leibfarth, F. A.; Oh, S.; Poelma, J. E.; Hawker, C. J.; Read de Alaniz, J. Photoswitching using visible light: a new class of organic photochromic molecules. *J. Am. Chem. Soc.* **2014**, *136*, 8169-8172; (b) Helmy, S.; Oh, S.; Leibfarth, F. A.; Hawker, C. J.; Read de Alaniz, J. Design and synthesis of donor-acceptor stenhouse adducts: a visible light photoswitch derived from furfural. *J. Org. Chem.* **2014**, *79*, 11316-11329.

(5) (a) Balamurugan, A.; Lee, H.-i. A visible light responsive on-off polymeric photoswitch for the colorimetric detection of nerve agent mimics in solution and in the vapor phase. *Macromolecules* **2016**, *49*, 2568-2574; (b) Singh, S.; Friedel, K.; Himmerlich, M.; Lei, Y.; Schlingloff, G.; Schober, A. Spatiotemporal photopatterning on polycarbonate surface through visible light responsive polymer bound DASA compounds. *ACS Macro Lett.* **2015**, *4*, 1273-1277; (c)

Poelma, S. O.; Oh, S. S.; Helmy, S.; Knight, A. S.; Burnett, G. L.; Soh, H. T.; Hawker, C. J.; de Alaniz, J. R. Controlled drug release to cancer cells from modular one-photon visible light-responsive micellar system. *Chem. Commun.* **2016**, *52*, 10525-10528; (d) Mason, B.; Whittaker, M.; Hemmer, J.; Arora, S.; Harper, A.; Alnemrat, S.; McEachen, A.; Helmy, S.; Read de Alaniz, J.; Hooper, J. A

temperature-mapping molecular sensor for polyurethane-based elastomers. *Appl. Phys. Lett.* **2016**, *108*, 041906.

(6) (a) Mallo, N.; Brown, P. T.; Iranmanesh, H.; MacDonald, T. S.; Teusner, M. J.; Harper, J. B.; Ball, G. E.; Beves, J. E. Photochromic switching behaviour of donor-acceptor Stenhouse adducts in organic solvents. *Chem. Commun.* **2016**, *52*, 13576-13579; (b) Mallo, N.; Foley, E. D.; Iranmanesh, H.; Kennedy, A. D.; Luis, E. T.; Ho, J.; Harper, J. B.; Beves, J. E. Structure-function relationships of donor-acceptor Stenhouse adduct photochromic switches. *Chem. Sci.* **2018**, *9*, 8242-8252; (c) Lerch, M. M.; Wezenberg, S. J.; Szymanski, W.; Feringa, B. L. Unraveling the photoswitching mechanism in donor-acceptor stenhouse adducts. *J. Am. Chem. Soc.* **2016**, *138*, 6344-6347.

(7) (a) Mal, P.; Breiner, B.; Rissanen, K.; Nitschke, J. R. White phosphorus is air-stable within a self-assembled tetrahedral capsule. *Science* **2009**, *324*, 1697-1699; (b) Takezawa, H.; Akiba, S.; Murase, T.; Fujita, M. Cavity-directed chromism of phthalein dyes. *J. Am. Chem. Soc.* **2015**, *137*, 7043-7046; (c) Samanta, D.; Galaktionova, D.; Gemen, J.; Shimon, L. J.; Diskin-Posner, Y.; Avram, L.; Král, P.; Klajn, R. Reversible chromism of spiropyran in the cavity of a flexible coordination cage *Nature communications* **2018**, *9*, 641

(8) (a) Seidel, S. R.; Stang, P. J. High-symmetry coordination cages via self-assembly. *Acc. Chem. Res.* **2002**, *35*, 972-983; (b) Mishra, A.; Dubey, A.; Min, J. W.; Kim, H.; Stang, P. J.; Chi, K.-W. Molecular self-assembly of arene-Ru based interlocked catenane metalla-cages. *Chem. Commun.* **2014**, *50*, 7542-7544; (c) Pollock, J. B.; Cook, T. R.; Stang, P. J. Photophysical and computational investigations of bis (phosphine) organoplatinum (II) metallacycles. *J. Am. Chem. Soc.* **2012**, *134*, 10607-10620; (d) Sun, Q. F.; Murase, T.; Sato, S.; Fujita, M. A Sphere-in-Sphere Complex by Orthogonal Self-Assembly. *Angew. Chem., Int. Ed.* **2011**, *50*, 10318-10321; (e) Fujita, M.; Tominaga, M.; Hori, A.; Therrien, B.

Coordination assemblies from a Pd (II)-cornered square complex. *Acc. Chem. Res.* **2005**, *38*, 369-378; (f) Wood, C. S.; Ronson, T. K.; Belenguer, A. M.; Holstein, J. J.; Nitschke, J. R. Two-stage directed self-assembly of a cyclic [3] catenane. *Nat. Chem.* **2015**, *7*, 354; (g) Hardy, M.; Struch, N.; Topić, F.; Schnakenburg, G.; Rissanen, K.; Lützen, A. Stepwise Construction of Heterobimetallic Cages by an Extended Molecular Library Approach. *Inorg. Chem.* **2017**, *57*, 3507-3515; (h) Mittal, N.; Saha, M. L.; Schmittel, M. A seven-component metallosupramolecular quadrilateral with four different orthogonal complexation vertices. *Chem. Commun.* **2015**, *51*, 15514-15517;

(i) Huang, C.-B.; Xu, L.; Zhu, J.-L.; Wang, Y.-X.; Sun, B.; Li, X.; Yang, H.-B. Real-time monitoring the dynamics of coordination-driven self-assembly by fluorescence-resonance energy transfer. *J. Am. Chem. Soc.* **2017**, *139*, 9459-9462; (j) Jiang, B.; Chen, L.-J.; Xu, L.; Liu, S.-Y.; Yang, H.-B. A series of new star-shaped or branched platinum-acetylide derivatives: synthesis, characterization, and their aggregation behavior. *Chem. Commun.* **2013**, *49*, 6977-6979; (k) Yan, X.; Wang, H.; Hauke, C. E.; Cook, T. R.; Wang, M.; Saha, M. L.; Zhou, Z.; Zhang, M.; Li, X.; Huang, F. A suite of tetraphenylethylene-based discrete organoplatinum (II) metallacycles: Controllable structure and stoichiometry, aggregation-induced emission, and nitroaromatics sensing. *J. Am. Chem. Soc.* **2015**, *137*, 15276-15286; (l) Fan, W. J.; Sun, B.; Ma, J.; Li, X.; Tan, H.; Xu, L. Coordination-Driven Self-Assembly of Carbazole-Based Metallodendrimers with Generation-Dependent Aggregation-Induced Emission Behavior. *Chem. Eur. J.* **2015**, *21*, 12947-12959; (m) Wei, P.; Yan, X.; Huang, F. Supramolecular polymers constructed by orthogonal self-assembly based on host-guest and metal-ligand interactions. *Chem. Soc. Rev.* **2015**, *44*, 815-832; (n) Komine, S.; Takahashi, S.; Kojima, T.; Sato, H.; Hiraoka, S. Self-assembly processes of octahedron-shaped Pd<sub>6</sub>L<sub>4</sub> cages. *J. Am. Chem. Soc.* **2019**, *141*, 3178-3186; (o) Li, E.; Jie, K.; Zhou, Y.; Zhao, R.; Huang, F. Post-Synthetic Modification of Nonporous Adaptive Crystals of Pillar [4] arene [1] quinone by Capturing Vaporized Amines. *J. Am. Chem. Soc.* **2018**, *140*, 15070-15079; (p) Shi, B.; Liu, Y.; Zhu, H.; Vanderlinden, R. T.; Shangguan, L.; Ni, R.; Acharyya, K.; Tang, J.; Zhou, Z.; Li, X.; Huang, F.; Stang, P. J. Spontaneous Formation of a Cross-Linked Supramolecular Polymer Both in the Solid State and in

Solution Driven by Platinum (II) Metallacycle-Based Host–Guest Interactions *J. Am. Chem. Soc.* **2019**, *141*, 6494-6496.

(9) (a) Chakrabarty, R.; Mukherjee, P. S.; Stang, P. J. Supramolecular coordination: self-assembly of finite two- and three-dimensional ensembles. *Chem. Rev.* **2011**, *111*, 6810-6918; (b) Cook, T. R.; Stang, P. J. Recent developments in the preparation and chemistry of metallacycles and metallacages via coordination. *Chem. Rev.* **2015**, *115*, 7001-7045; (c) Forgan, R. S.; Sauvage, J.-P.; Stoddart, J. F. Chemical topology: complex molecular knots, links, and entanglements. *Chem. Rev.* **2011**, *111*, 5434-5464; (d) McConnell, A. J.; Wood, C. S.; Neelakandan, P. P.; Nitschke, J. R. Stimuli-responsive metal–ligand assemblies. *Chem. Rev.* **2015**, *115*, 7729-7793; (e) Mukherjee, S.; Mukherjee, P. S. Template-free multicomponent coordination-driven self-assembly of Pd (II)/Pt (II) molecular cages. *Chem. Commun.* **2014**, *50*, 2239-2248.

(10) (a) Howlader, P.; Mondal, B.; Purba, P. C.; Zangrando, E.; Mukherjee, P. S. Self-Assembled Pd (II) Barrels as Containers for Transient Merocyanine Form and Reverse Thermochromism of Spiropyran. *J. Am. Chem. Soc.* **2018**, *140*, 7952-7960; (b) Brenner, W.; Ronson, T. K.; Nitschke, J. R. Separation and selective formation of fullerene adducts within an M18L6 cage. *J. Am. Chem. Soc.* **2016**, *139*, 75-78; (c) Anhäuser, J.; Puttreddy, R.; Lorenz, Y.; Schneider, A.; Engeser, M.; Rissanen, K.; Lützen, A. Chiral self-sorting behaviour of [2.2] paracyclophane-based bis (pyridine) ligands. *Org. Chem. Front.*, **2019**, *6*, 1226-1235; (d) Biswas, P. K.; Saha, S.; Paululat, T.; Schmittel, M. Rotating catalysts are superior: suppressing product inhibition by anchimeric assistance in four-component catalytic machinery. *J. Am. Chem. Soc.* **2018**, *140*, 9038-9041.

(11) Luo, L.; Wang, P.; Xu, G.-C.; Liu, Q.; Chen, K.; Lu, Y.; Zhao, Y.; Sun, W.-Y. Zinc (II) and cadmium (II) complexes with rigid 3, 3', 5, 5'-tetra (1H-imidazol-1-yl)-1, 1'-biphenyl and varied carboxylate ligands. *Crystal Growth & Design* **2012**, *12*, 2634-2645.

(12) (a) Singh, G. S.; Desta, Z. Y. Isatins as privileged molecules in design and synthesis of spiro-fused cyclic frameworks. *Chem. Rev.* **2012**, *112*, 6104-6155; (b) Pizzirani, D.; Roberti, M.; Grimaudo, S.; Di Cristina, A.; Pipitone, R. M.; Tolomeo, M.; Recanatini, M. Identification of biphenyl-based hybrid molecules able to decrease the intracellular level of Bcl-2 protein in Bcl-2 overexpressing leukemia cells. *Journal of medicinal chemistry* **2009**, *52*, 6936-6940.

(13) (a) Amireddy, M.; Chen, K. Organocatalytic synthesis of spirocyclohexane indane-1, 3-diones via a chiral squaramide-catalyzed Michael/aldol cascade reaction of  $\gamma$ -nitro ketones and 2-arylideneindane-1, 3-diones. *Tetrahedron* **2015**, *71*, 8003-8008; (b) Duan, H.; Chen, Z.; Han, L.; Feng, Y.; Zhu, Y.; Yang, S. Palladium-catalyzed chemoselective synthesis of indane-1, 3-dione derivatives via tert-butyl isocyanide insertion. *Org. Biomol. Chem.* **2015**, *13*, 6782-6788.

(14) (a) Sheldrick, G. SHELXTL-Plus. Program for the Solution and Refinement of Crystal Structures *Bruker Analytical X-Ray Systems, Madison, Wisconsin, USA* **1998**; (b) Farrugia, L. WinGX version 1.64, an integrated system of windows programs for the solution, refinement and analysis of single-crystal X-ray diffraction data *University of Glasgow, Glasgow* **2003**; (c) Farrugia, L. J. WinGX suite for small-molecule single-crystal crystallography *J. Appl. Crystallogr.* **1999**, *32*, 837-838.

(15) Sheldrick, G. M. SHELXT—Integrated space-group and crystal-structure determination *Acta Crystallographica Section A: Foundations and Advances* **2015**, *71*, 3-8.

# Unusual Behaviour of Donor-Acceptor Stenhouse Adducts (DASA) in Confined Space of a Water Soluble Pd<sup>II</sup><sub>8</sub> Molecular Vessel

Rupak Saha<sup>1</sup>, Anthonisamy Devaraj<sup>1§</sup>, Soumalya Bhattacharyya<sup>1§</sup>, Soumik Das<sup>1</sup>, Ennio Zangrando<sup>2</sup> and Partha Sarathi Mukherjee<sup>1\*</sup>

